13th International Symposium on Turbulence and Shear Flow Phenomena (TSFP13)
Montreal, Canada, June 25–28, 2024

EXTREME AERODYNAMICS OF VORTEX IMPINGEMENT: MACHINE-LEARNING-BASED COMPRESSION AND SITUATIONAL AWARENESS

Kai Fukami and Kunihiko Taira
Department of Mechanical and Aerospace Engineering, University of California, Los Angeles, CA 90095, USA
kfukami1@g.ucla.edu and ktaira@seas.ucla.edu

ABSTRACT

Gaining accurate awareness of the global dynamical state from sparse measurements is an overarching challenge in science and engineering. This challenging inverse problem becomes especially complicated for small-scale modern air vehicles that fly in extreme aerodynamic conditions. This study shows that real-time situational awareness can be achieved even under extremely gusty conditions by leveraging an observable-augmented machine-learning technique. We further find that nonlinear machine learning offers a low-dimensional, physically-interpretable manifold space that captures the essence of high-dimensional extreme aerodynamics. The proposed data-driven techniques can support next-generation air vehicles that are required to fly in operating extreme environments encountered in urban canyons and mountainous areas in severe weather.

INTRODUCTION

Small-scale air vehicles are tasked to navigate in complex airspace such as urban and mountainous areas as well as turbulent wakes created by ships in adverse weather to support search, transport, and defense operations. Under such conditions, small air vehicles encounter extremely strong gusts that have traditionally been avoided due to their inability to sustain flight operations (Jones *et al.*, 2022). Extreme aerodynamics related to gusts are characterized by a large number of parameters, which makes parameter sweeps with expensive numerical simulations and experiments impractical. Furthermore, theoretical analyses face a significant challenge due to the strongly nonlinear nature of the extreme aerodynamics (Fukami *et al.*, 2024).

To tackle this challenge, we develop a data-driven approach for real-time situational awareness under extremely unsteady flight environments, while identifying a physically-interpretable low-dimensional manifold of high-dimensional aerodynamics. The present observable-augmented neural network can be leveraged not only to understand the rich physics of extreme aerodynamic flows on the identified manifold but also to compress high-dimensional physics into a very small number of variables, which is critical towards real-time control of the vehicle.

METHODS

The goal of the present study is to reconstruct extreme aerodynamic flows from sparse measurements in a computationally efficient manner while also providing a low-rank and interpretable description of high-dimensional complex wake physics. The overview of the present study is illustrated in figure 1(a). The present formulation is composed of three steps: 1. identification of a low-dimensional manifold using a lift-augmented convolutional autoencoder, 2. estimation of latent vectors in the manifold space from sparse pressure measurements using a multi-layer perceptron, and 3. reconstruction of extreme aerodynamic flows from these sparse pressure sensors. In what follows, we provide details for each step of the present approach.

As a model of extreme aerodynamic problems, we consider a severe gust-vortex wing interaction, causing strong nonlinearities in a flow field. This can emulate challenging flight conditions observed in a wide range of realistic flow situations. We generate numerical data sets covering a variety of wake patterns around a NACA0012 airfoil at a Reynolds number $Re = 100$ using an incompressible flow solver (Ham & Iaccarino, 2004; Ham *et al.*, 2006). The simulated flows are validated with previous studies (Zhong *et al.*, 2023; Kurtulus, 2015; Liu *et al.*, 2012; Di Ilio *et al.*, 2018). Representative vortical flows and time series of lift forces are shown in figure 1(b). We consider angles of attack $\alpha \in [20^\circ, 60^\circ]$. For the undisturbed cases shown in the dotted boxes for each angle in figure 1(b), the wakes at $\alpha \leq 20^\circ$ present steady (no-shedding) flow, while those for $\alpha \geq 30^\circ$ exhibit periodic shedding behavior that correspond to periodic limit cycles.

In addition to the undisturbed cases, the present data set includes a large number of extreme aerodynamic cases associated with strong vortex disturbance interacting with the wing. A single vortex gust modeled by a Taylor vortex (Taylor, 1918), $u_\theta = u_{\theta,\max}(r/R)\exp[1/2 - r^2/(2R^2)]$, where the radius of the vortex is R, is initially introduced upstream of the wing at $(x_0/c, y_0/c)$ with x_0/c being -2. This can model an extreme vortex disturbance hitting a wing during flight. The present disturbance vortex is parameterized by the gust ratio $G \equiv u_{\theta,\max}/u_\infty \in [-10, 10]$, its diameter $D \equiv 2R/c \in [0.5, 2]$, and the vertical position of the disturbance $Y \equiv y_0/c \in [-0.5, 0.5]$. Here, u_∞ is the free-stream velocity and c is the chord length. It is worth pointing out that the conditions of $G \gtrsim 1$ are traditionally considered difficult for stable flight (Jones *et al.*, 2022). Hence, the presently considered conditions of $G \gtrsim 1$ are extremely challenging to sustain flight. Vortex gusts appearing in the actual atmosphere can be more complex due to a higher Re than our consideration here. Note, however, that the current setup captures the dominant interaction dynamics between large vortex core and the airfoil in a two-dimensional manner since the large vorticity source from the surface under local flow acceleration can be resolved.

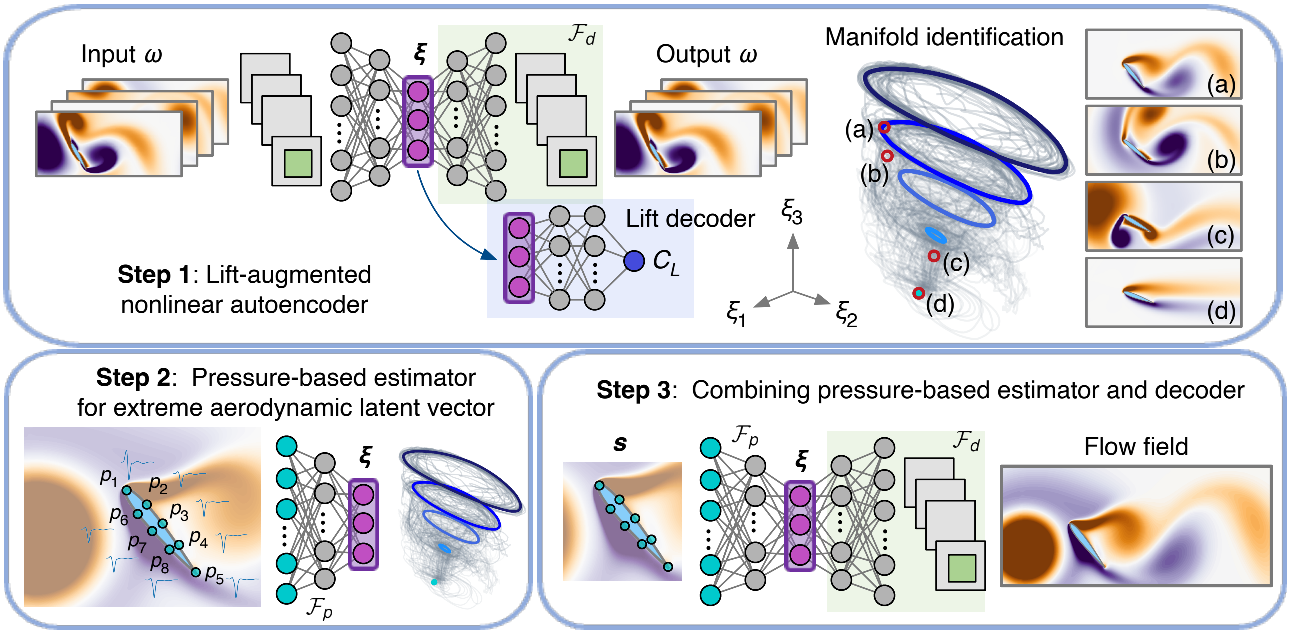

Figure 1. Overview of the present study. We first extract a low-dimensional representation of high-dimensional extreme aerodynamics as the latent vector $\boldsymbol{\xi}$ using a lift-augmented nonlinear autoencoder (step 1). We then construct another network to estimate latent vectors on the identified manifold from pressure measurements on the airfoil surface (step 2). The decoder part in step 1 and the pressure-based estimator in step 2 are finally combined to reconstruct a high-dimensional flow state $\boldsymbol{\omega}$ from sparse sensors (step 3).

We simulate 40 cases of disturbed flows for each angle of attack with randomly sampled parameters composed of the aforementioned three variables shown at the bottom right in figure 1(b). For the present analysis, we use 20 cases per angle of attack for training of models while the remaining 20 cases are used for testing. Furthermore, the time history of the lift coefficients C_L is prepared, which will be used for the present physics-inspired model design. The present training data set is comprised of 1.26×10^5 snapshots from 100 extreme aerodynamic cases and 5 undisturbed wake cases. Each case includes 1200 snapshots, resulting in an extremely large spatiotemporal degree of freedom of $\mathscr{O}(10^9)$. We develop in this study a universal approximator that estimates the high-dimensional and rich aerodynamic flows from sparse surface pressure sensors. This is achieved while identifying a three-dimensional coordinate that captures extremely violent aerodynamic effects in a tractable manner.

The first step of the present approach is to find appropriate low-dimensional coordinates that best describe high-dimensional extreme aerodynamic vortical flows $\boldsymbol{\omega}$. However, traditional linear dimensionality reduction techniques have difficulty in compressing transient physics observed in the present data. Hence, this study considers nonlinear compression assisted with a convolutional autoencoder (Hinton & Salakhutdinov, 2006; LeCun *et al.*, 1998). An autoencoder outputs the same data as the given input through a low-dimensional subspace using nonlinear activation functions. The latent vector $\boldsymbol{\xi}$ (purple circles in figure 1(a)) can be regarded as a low-dimensional representation of the given data if the model successfully provides the output data that accurately approximates the input data. Here, we found the optimal latent variable size to be 3.

While efficient data compression can be achieved with a naïve nonlinear autoencoder (Milano & Koumoutsakos, 2002; Murata *et al.*, 2020), this study seeks coordinates that express the disturbed wake dynamics in a physically-interpretable subspace. For this reason, we propose a lift-augmented autoencoder which includes additional layers based on multi-layer perceptron (MLP) (Rumelhart *et al.*, 1986) to produce the lift response C_L as an augmented output from the latent vector $\boldsymbol{\xi}$, as illustrated in figure 1(a). Since the present model needs to compress the high-dimensional vortical flows $\boldsymbol{\omega}$ while producing the lift coefficient C_L, we can promote the identification of the appropriate latent variable coordinates that respect the correlation between $\boldsymbol{\omega}$ and C_L. We note that this choice of C_L for the model augmentation is inspired by our theoretical knowledge that vorticity field and its spatial arrangement are responsible for exerting lift on a wing.

The optimization of the present autoencoder is expressed as

$$\boldsymbol{w}_a^* = \mathrm{argmin}_{\boldsymbol{w}_a}\left[||\boldsymbol{\omega} - \hat{\boldsymbol{\omega}}||_2 + \beta||C_L - \hat{C_L}||_2\right], \qquad (1)$$

where $\boldsymbol{w}_a$ denotes the weights inside the autoencoder model and β balances the reconstruction loss and the lift-based loss.

Next, we estimate the identified latent space manifold $\boldsymbol{\xi}(t)$ from pressure sensor measurements $\boldsymbol{s}(t)$, in step 2 of figure 1(a). We place 8 sensors around a wing in an equispaced manner. Since this estimation is a transformation of $\mathbb{R}^8 \to \mathbb{R}^3$, we here use an MLP. The weights $\boldsymbol{w}_p$ of the MLP-based manifold estimator $\mathscr{F}_p$ are optimized through

$$\boldsymbol{w}_p^* = \mathrm{argmin}_{\boldsymbol{w}_p}||\boldsymbol{\xi} - \mathscr{F}_p(\boldsymbol{s};\boldsymbol{w}_p)||_2. \qquad (2)$$

A combination of the decoder $\mathscr{F}_d$ of the autoencoder and the manifold estimator $\mathscr{F}_p$ enables us to directly estimate a high-dimensional vortical flow $\hat{\boldsymbol{\omega}}_p(t)$ from pressure sensors $\boldsymbol{s}(t)$ without necessitating the retraining of machine-learning models. The present manifold identification promotes robustness against unseen (testing) data in reconstructing extreme aerodynamic flows since the present lift-augmented autoencoder

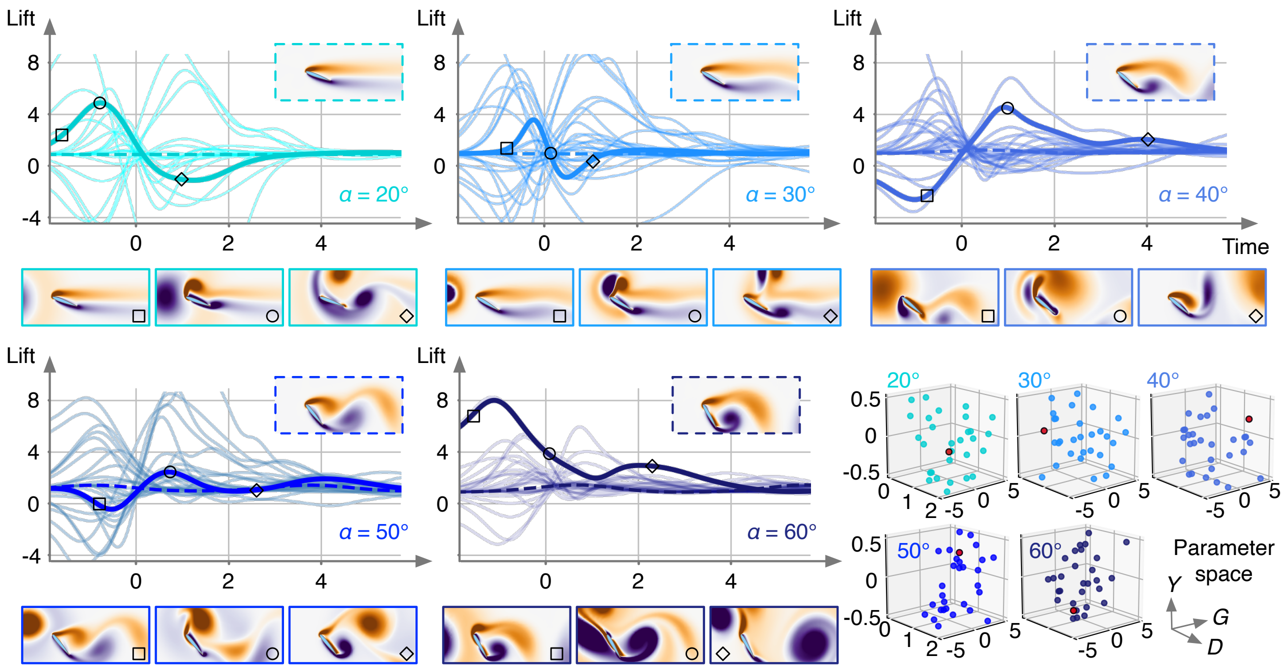

Figure 2. Extreme aerodynamic data sets. All lift responses for angles of attack of $\alpha \in [20^\circ, 60^\circ]$ are shown. Representative vorticity fields ω are shown at three time instances (□, ○, and ◇). The vorticity field surrounded by the dotted line is the undisturbed reference flow for each angle of attack. The red circles in the parameter spaces correspond to the representative cases chosen for the vorticity visualization.

can map a variety of wake features that commonly appear in vortical flows into a low-order space. This reconstruction stage (step 3 in figure 1(a)) can be expressed as

$$\omega \approx \hat{\omega}_p = \mathscr{F}_d(\mathscr{F}_p(\boldsymbol{s}; \boldsymbol{w}_p); \boldsymbol{w}_A). \tag{3}$$

The present formulation offers a physically guided process of a machine-learning-based flow estimation, avoiding a black-box learning process.

RESULTS

Let us first discuss the low-dimensional manifold identification via the lift-augmented autoencoder. The three-dimensional feature space and decoded variables are shown in figure 1(c1-c3). For comparison, we additionally consider linear PCA (Jolliffe, 2002) and a regular autoencoder. As shown, the low-dimensional PCA subspace is unable to distinguish the undisturbed wakes and the projections of all disturbed cases (gray lines). In fact, the PCA encounters difficulty in reconstructing the flow state, yielding almost 100% error. This clearly indicates that the three coefficients produced by the linear technique are not enough to express the entire physics covering a huge parameter space of extreme aerodynamics.

This issue of data compressibility can be mitigated with a nonlinear autoencoder, exhibiting drastically improved reconstruction, as shown in figure 1(c). However, the latent vector of this autoencoder for disturbed flows appears unorganized, because the model uses the latent space to distinguish a variety of the wake scenarios in minimizing the reconstruction loss.

Next, let us consider the present lift-augmented autoencoder which discovers a physically coherent low-dimensional expression while reconstructing the flow variables well, as shown figure 1(c). The latent vectors of the undisturbed baseline flows highlighted in color capture the hierarchical relationship of the induced angle of attack in the ξ_3 direction. While the case of $\alpha = 20^\circ$ is expressed as a single dot, the cases with unsteady periodic shedding of $\alpha \geq 30^\circ$ are mapped as circles. This represents the steady and unsteady limit-cycle oscillations in a high-dimensional state. Further, the radius of the circles for the cases of $\alpha \geq 30^\circ$ increases with the angle, corresponding to the increment in the fluctuations from the mean state for each case of the angle of attacks. Note that the disturbed wake can be expressed about the undisturbed orbit, as shown in figure 1(c). This suggests that the discovered manifold expresses how the extreme disturbance affects the undisturbed baseline dynamics in a low-order manner.

The latent vector $\boldsymbol{\xi}$ on the discovered manifold can be estimated from sparse pressure sensors through the MLP-based estimator $\mathscr{F}_p$. These estimated latent vectors $\mathscr{F}_p(\boldsymbol{s})$ can be then provided to the decoder $\mathscr{F}_d$ of the aforementioned lift-augmented autoencoder to reconstruct extreme aerodynamic flows. Examples of reconstructed flows are depicted in figure 1(d). A variety of wake patterns can be accurately reconstructed from only eight sensor measurements. The present results suggest that real-time situational awareness under extreme aerodynamic conditions can be achieved by leveraging a physics-inspired data-driven approach.

CONCLUDING REMARKS

We presented an observable-augmented machine-learning technique. In particular, this study considered a lift-augmented autoencoder and a manifold estimator, which achieves real-time flow reconstruction from sparse measurements even under extreme aerodynamic flight conditions. Furthermore, we found that such seemingly complex extreme aerodynamics can be compressed into only three variables in a physically tractable manner. The present approach, which couples data-driven sensing with physically-interpretable manifold identification, has exciting potential to enable flight even under the most extreme aerodynamic conditions. Additional details

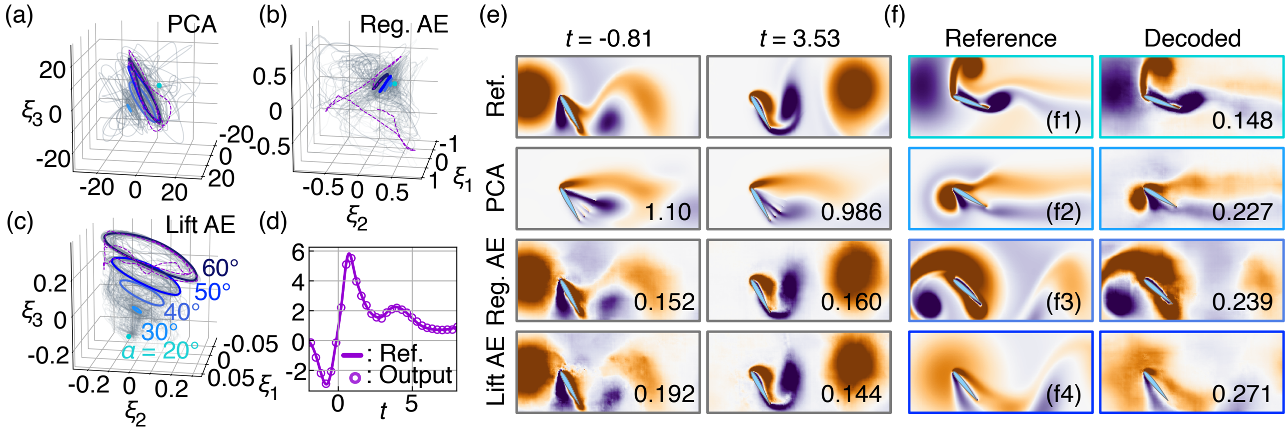

Figure 3. Three-dimensional latent space obtained by (a) PCA, (b) a regular autoencoder, and (c) the lift-augmented autoencoder. The undisturbed cases are highlighted in color. All disturbed wake cases used for training are also exhibited with light gray curves. The purple dotted line in each space corresponds to an example of the extreme aerodynamic flows with the parameter of $(\alpha, G, D, Y) = (60^\circ, -2.8, 0.75, 0)$. (d) Lift response and (e) reconstructed vorticity fields of the example case are also shown. The value on each contour reports an L_2 error norm $\varepsilon = ||\omega - \hat{\omega}||_2/||\omega||_2$. (f) Examples of reference vortical flows $\boldsymbol{\omega}$ and reconstructed vorticity fields $\hat{\omega}_p = \mathscr{F}_d(\mathscr{F}_p(\boldsymbol{s}; \boldsymbol{w}_p), \boldsymbol{w}_A)$ from pressure sensors. Examples of the extreme aerodynamic flows with the parameter of (α, G, D, Y); (f1) = $(20^\circ, 1.8, 2, 0.1)$ at $t = -0.725$, (f2) = $(30^\circ, -2.8, 0.5, -0.3)$ at $t = -0.125$, (f3) = $(40^\circ, -3.4, 1.5, 0)$ at $t = -0.125$, and (f4) = $(50^\circ, -1.2, 2, -0.1)$ at $t = -0.045$ are shown. The value on each contour reports an L_2 error norm $\varepsilon_p = ||\omega - \hat{\omega}_p||_2/||\omega||_2$.

on manifold identification are presented in Fukami & Taira (2023).

REFERENCES

Di Ilio, G., Chiappini, D., Ubertini, S., Bella, G. & Succi, S. 2018 Fluid flow around NACA 0012 airfoil at low-Reynolds numbers with hybrid lattice Boltzmann method. *Comput. Fluids* **166**, 200–208.

Fukami, K., Nakao, H. & Taira, K. 2024 Data-driven transient lift attenuation for extreme vortex gust-airfoil interactions. *arXiv:2403.00263* .

Fukami, K. & Taira, K. 2023 Grasping extreme aerodynamics on a low-dimensional manifold. *Nat. Commun.* **14**, 6480.

Ham, F. & Iaccarino, G. 2004 Energy conservation in collocated discretization schemes on unstructured meshes. In *Annual Research Briefs*, pp. 3–14. Center for Turbulence Research.

Ham, F., Mattsson, K. & Iaccarino, G. 2006 Accurate and stable finite volume operators for unstructured flow solvers. In *Annual Research Briefs*, pp. 243–261. Center for Turbulence Research.

Hinton, G. E. & Salakhutdinov, R. R. 2006 Reducing the dimensionality of data with neural networks. *Science* **313** (5786), 504–507.

Jolliffe, I. T. 2002 *Principal component analysis*. Springer.

Jones, A. R., Cetiner, O. & Smith, M. J. 2022 Physics and modeling of large flow disturbances: Discrete gust encounters for modern air vehicles. *Annu. Rev. Fluid Mech.* **54**, 469–493.

Kurtulus, D. F. 2015 On the unsteady behavior of the flow around NACA 0012 airfoil with steady external conditions at $Re = 1000$. *Int. J. Micro Air Veh.* **7** (3), 301–326.

LeCun, Y., Bottou, L., Bengio, Y. & Haffner, P. 1998 Gradient-based learning applied to document recognition. *Proc. IEEE* **86** (11), 2278–2324.

Liu, Y., Li, K., Zhang, J., Wang, H. & Liu, L. 2012 Numerical bifurcation analysis of static stall of airfoil and dynamic stall under unsteady perturbation. *Commun. Nonlinear Sci. Numer. Simul.* **17** (8), 3427–3434.

Milano, M. & Koumoutsakos, P. 2002 Neural network modeling for near wall turbulent flow. *J. Comput. Phys.* **182**, 1–26.

Murata, T., Fukami, K. & Fukagata, K. 2020 Nonlinear mode decomposition with convolutional neural networks for fluid dynamics. *J. Fluid Mech.* **882**, A13.

Rumelhart, D. E., Hinton, G. E. & Williams, R. J. 1986 Learning representations by back-propagation errors. *Nature* **322**, 533–536.

Taylor, G. I. 1918 On the dissipation of eddies. *Meteorology, Oceanography and Turbulent Flow* pp. 96–101.

Zhong, Y., Fukami, K., An, B. & Taira, K. 2023 Sparse sensor reconstruction of vortex-impinged airfoil wake with machine learning. *Theor. Comput. Fluid Dyn.* **37**, 269–287.